Thyroid tissue analysis through Raman spectroscopy†

Caroline S. B. Teixeira,‡*[a] Renata A. Bitar,‡[b] Herculano S. Martinho,‡[b] André B. O. Santos,[a] Marco A. V. Kulcsar,[a] Celso U. M. Friguglietti,[a] Ricardo B. da Costa,[a] Emilia Â. L. Arisawa[a] and Airton A. Martin[a]

Received 16th December 2008, Accepted 14th September 2009
First published as an Advance Article on the web 21st September 2009
DOI: 10.1039/b822578h

The diagnosis of thyroid pathologies is usually made by cytologic analysis of the fine needle aspiration (FNA) material. However, this procedure has a low sensitivity at times, presenting a variation of 2–37%. The application of optical spectroscopy in the characterization of alterations could result in the development of a minimally invasive and non-destructive method for the diagnosis of thyroid diseases. Thus, the objective of this work was to study the biochemical alterations of tissues and hormones (T3 and T4) of the thyroid gland by means of molecular vibrations probed by FT-Raman spectroscopy. Through the discriminative linear analysis of the Raman spectra of the tissue, it was possible to establish (in percentages) the correct classification index among the groups: goitre adjacent tissue, goitre nodular region, follicular adenoma, follicular carcinoma and papillary carcinoma. As a result of the comparison between the groups goitre adjacent tissue *versus* goitre nodular region, an index of 58.3% of correct classification was obtained; this percentage was considered low, and it was not possible to distinguish the Raman spectra of these groups. Between goitre (nodular region and adjacent tissue) *versus* papillary carcinoma, the index of correct classification was 64.9%, which was considered good. A relevant result was obtained in the analysis of the benign tissues (goitre and follicular adenoma) *versus* malignant tissues (papillary and follicular carcinomas), for which the index was 72.5% and considered good. It was also possible, by means of visual observation, to find similar vibrational modes in the hormones and pathologic tissues. In conclusion, some biochemical alterations, represented by the FT-Raman spectra, were identified that could possibly be used to classify histologic groups of the thyroid. However, more studies are necessary due to the difficulty in setting a standard for pathologic groups.

Introduction

The thyroid is considered the most important organ of endocrine function in the body. Its hormone secretions play an important role in the normal growth and development, as well as contributing to homeostasis, which controls heat and energy production. Any alteration in the synthesis and secretion of the thyroidal hormones can result in growth retardation, vascular diseases, lung and kidney dysfunctions, chronic constipation, neuromuscular alterations, central neural system related symptoms, and anaemia, among other related pathologies.[1] Apart from the complex hormonal action that is reflected in a secondary form in many organs of the body, the gland itself can be injured; for example, neoplasias, which have been considered more important, can damage the gland and are more difficult to diagnose.

The thyroid is one of the most reactive organs of the body and, of all the endocrine glands, is the one that contains the most important hormones. The thyroid responds to many stimuli and is in a constant state of adaptation. During puberty, pregnancy and psychological stress of any description, the gland increases its size and becomes more active. This functional instability reflects on the hyperplasia of the thyroidal epithelium. At that moment, the thyroglobulin is re-absorbed, and the follicle cells become higher and columnar, sometimes forming small crooked buttons or papilla. When the stress disappears the involution of the gland occurs; that is, the height of the epithelium decreases, colloid accumulates and the follicle cells regain their normal shape and size. Alterations in this equilibrium between hyperplasia and involution could cause changes, accentuated or not, in the normal histologic standard.[2]

The occurrence rate of the thyroidal palpable nodule, in general, is between 4% and 7%; however, with the advent of the ultrasonography, the occurrence increases to 30%, proving the high mitogenic capacity of the tissue. The nodules are mostly benign injures, either toxic or non-toxic, such as the colloid goitre or follicular adenomas, and only a small amount corresponds to

[a]*Universidade do Vale do Paraíba/Instituto de Pesquisa e Desenvolvimento - Laboratório de Espectroscopia Vibracional Biomédica, Av. Shishima Hifumi 2911, Urbanova, CEP 12244-000 São José dos Campos, São Paulo, Brazil. E-mail: carolsbt@uol.com.br; Tel: +55 12 3947-116*
[b]*Centro de Ciências Naturais e Humanas, Universidade Federal do ABC, 09090-400 Santo André, São Paulo, Brazil*

† This paper was submitted as part of an *Analyst* themed issue on Optical Diagnosis. The issue includes work which was presented at SPEC 2008 Shedding Light on Disease: Optical Diagnosis for the New Millennium, which was held in São José dos Campos, São Paulo, Brazil, October 25–29, 2008. Other papers on this topic can be found in issue 6 of vol. 134 (2009). This issue can be found from the *Analyst* homepage (http://www.rsc.org/analyst).

‡ Equally contributed to the work.

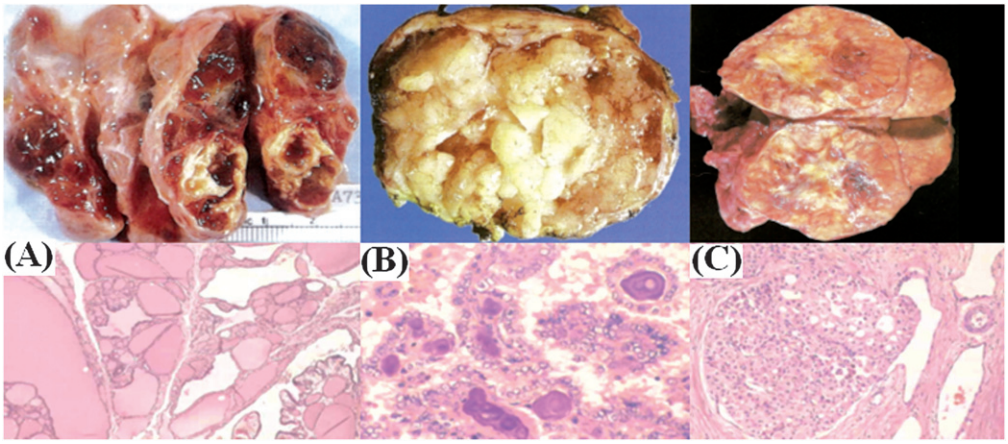

Fig. 1 (A) Nodular goitre: the gland shows rough nodules and contains fibrous areas and cystic alterations. (B) Thyroid papillary carcinoma: it contains well-formed papillae covered in cells for which the nuclei appear to be hollow, called nuclei in 'orphan Annie eye'. (C) Follicular carcinoma: the tumour has a pale beige colour and contains small haemorrhage focuses. (Adaptation based on ref. 2. Copyright 1984, WB Saunders.)

cancer. The thyroidal carcinomas have their origin in two types of cells: medullary carcinoma, originating from the parafollicular cells; and neoplasias of the follicular epithelium, with around 1% corresponding to anaplastic carcinoma, the most deadly thyroidal follicular carcinoma (Fig. 1). The Hürthle adenomas and carcinomas, also of follicular origin, represent the most common form of endocrine neoplasia.[3]

The diagnosis of thyroid pathologies usually occurs in the following order: anamnesis, ultrasonography and laboratory exams. Recently, a fine needle aspiration (FNA) could be required, where the cells collected are cytologically analysed. From the FNA, if the suspected malignancy is confirmed, a surgical procedure (partial or total thyroidectomy) is advised so that, after the material is sent for histologic analysis (anatomical pathologic analysis), the medical diagnostic can be concluded.

FNA is currently the most accepted procedure for diagnosing thyroid injuries, as it is a very useful and cost-effective tool. However, the sensitivity of this procedure for the thyroid is at times poor, with a high rate of false-negative results, and the variation ranges from 2% to 37%.[4] The differentiation of hyperplastic nodule (goitre), follicular adenoma or follicular carcinoma is difficult. The accuracy of the method is doubtful in these cases, and other alternatives and further methods are necessary to make the diagnosis more precise for such obscure injuries to the cytopathologic diagnosis.[4] False-negative results occur due to an ordinary mistake in sampling, which may occur in small tumours and samples associated with inflammations and degenerative changes next to the thyroidal parenchyma. In addition, some groups of injuries are difficult to interpret as being malignant or benign, and thus, the follicular injuries of colloid goitre are difficult to determine. The cytopathologic diagnoses of follicular adenoma and follicular carcinoma are complicated due to the fact that they depend on the histologic access to the capsular and vascular invasion perception. It is, therefore, vital to find new ways to detect the biochemical and cellular changes, in order to perfect the diagnosis and prognosis of thyroidal diseases. This is especially essential where the cytological diagnosis fails because the tumour cells were not extracted *via* FNA, and the cancer remains undiagnosed.[5]

It is important to note that at times the incorrect diagnosis leads the patient to surgery without appropriate urgency and indication. Because of its complex function, the thyroid has infinite controversies since the diagnosis until the medical opinion, not only regarding the cytologic and histologic analyses, but also regarding the clinical conduct (hormone regulation) and surgical procedure (partial or total thyroidectomy). As for the histologic difficulty, the fact is justified by the interpretative similarity of the tissue and its pathologies. According to Hedinger *et al.*,[6] there are variations among the thyroidal diseases, and the pleomorphism of the follicular cells can be contradictory when indicating malignancy. These cells are characterised by nuclear alterations in shape and size that become hyperchromatic. This can occur in hyperplasias, chronic thyroiditis, and in glands that might have been exposed to external radiation or radiotherapy.[6]

Considering the variations of the thyroid diseases and the difficulty of the morphologic diagnosis, the necessity of further techniques to distinguish benign and malignant characteristics of the thyroid lesion is evident. It is known that these diseases, with no exception, are caused by biochemical changes in the cells and/or tissues. Thus, the current challenge of modern medicine is to find an analytic technique that investigates these alterations through minimally invasive and non-destructive methods. Few analytic methods fulfil these requirements and are sensitive enough to reveal details of the biochemical composition and structure.[7]

Among the new techniques recently presented, optical biopsy by Raman spectroscopy is one of the most promising ones, due to the biochemical alterations that can be detected by the optical spectroscopy through the disease's characteristic spectral signs. This study was intended to reduce the disadvantages of the conventional biopsy and aimed to analyse the biochemical alterations in thyroidal tissues through Raman spectroscopy. In addition, an analysis of the synthetic thyroid hormones (T3 and T4) was performed, with the purpose of characterizing them in the spectra of tissues with pathologic alterations. Different aspects could be detected by the Raman spectroscopy method that can contribute and complement the clinic diagnosis of thyroidal pathologies.

Materials and methods

The experimental procedure was submitted to analysis and accepted by the Research Ethics Committee under protocol number H281/CEP/2007. All patients agreed to provide thyroid fragments for this research under Post-Informed Consent.

After the surgical procedure (thyroidectomy), 27 fragments of the thyroid were collected from 18 patients, comprising the following histologic groups: goitre adjacent tissue, goitre nodular tissue, follicular adenoma, follicular carcinoma and papillary carcinoma. The removed samples were conserved in Nalgene® cryogenic tubes in liquid nitrogen (−196 °C) until the spectroscopic analysis.

For the FT-Raman experiment, the samples were thawed in physiologic saline (0.9%) at room temperature, cut into fragments with scalpel blade number 15 (2 mm diameter), and positioned in the centre of an aluminium sample holder for the spectral acquisition. The equipment utilised was an FT-Raman spectrometer (Bruker RFS 100/S; Bruker Optics GmbH, Ettlingen, Germany), with an Nd-YAG excitation laser centred at 1064 nm, with an output power of 300 mW. The laser spot had a 0.6 mm diameter. For the experiment, 600 scans were performed, with spectral resolution of 4 cm^{-1}.

Three spectra of each fragment were collected, totalling 81 spectra. After the experiments, the same fragments were stocked in 10% formaldehyde and submitted to the standard procedure of lamination HE. In order to confirm the diagnosis, the samples were then sent to two pathologists for histopathology evaluation, according to the Brazilian Society of Clinical Pathology thyroid neoplasia diagnosis criteria. The results are shown in Table 1.

All the spectra were pre-processed automatically using a routine constructed in the software Matlab 6.1. (Vanderbilt University, Tennessee, USA). The procedure included in this routine involved the calculation of the moving average and the use of the fifth-degree polynomial to subtract the baseline, followed by vector normalization. The statistical analysis was performed using the software Minitab.

The corresponding assigned Raman bands were displayed in Tables 2, 3, 4, and 5. It was considered only those bands which presented greater than 20% of inter-group relative intensity variation. Moreover, only Raman bands were considered that had been previously reported in the literature. Thus, noise peaks or meaningless bands were automatically excluded since these are random events not present in all experimental groups.

For comparative purposes the Raman spectra of Liothyronine sodium (T3) and Levothyroxine sodium (T4) synthetic hormones were also studied. These were obtained commercially from the supplier Pharma Nostra. The synthetic T3 and T4 hormones in powder form were placed in the 2 mm diameter gap of an aluminium sample holder. Two spectra were collected, one for each hormone, in the 400–1800 cm^{-1} FT-Raman band. The parameters used for each of the spectra were as follows: 100 mW output power of the excitation laser (Nd:YAG), 200 scans, laser beam width of 0.5 mm, and spectral resolution of 1 cm^{-1}. The pre-processing of the spectra was also performed with the Matlab 6.1 routine. For the FT-Raman band at 400–1800 cm^{-1}, the baseline was corrected using a second-degree polynomial. It was then possible to construct a chart where the relevant vibrational modes in the differentiation of the hormones were related (Table 5), when comparing the spectral data of the pathologic tissues.

Table 1 Relation between final histopathologic report, number of samples and spectra acquired per sample

Sample type	Samples	Spectra
Goitre adjacent tissue	11	*33*
Goitre nodular region	9	*27*
Follicular adenoma	1	*3*
Papillary carcinoma	5	*15*
Follicular carcinoma	1	*3*
Total	***27***	***81***

Table 2 Vibrational modes in the differentiation of the injury adjacent tissue and goitre nodular region[10]

Peak (cm^{-1})		Assignment	Pathology
1[a]	540–800	Nucleic acids, nucleotides	Goitre adjacent tissue
2	856–930	Amino acid side chain vibrations of proline and hydroxyproline, as well as a (C–C) vibration of the collagen backbone; hydroxyproline (collagen type I)	Goitre nodular region
3	960	Symmetric stretching vibration of PO_4^{3-}; calcium phosphate stretch band; quinoid ring in-plane deformation	Goitre nodular region
4	1087–1090	C–C stretch; PO^{2-}; symmetric phosphate stretching vibrations	Goitre adjacent tissue
5	1246–1270	Amide III (collagen and proteins)	Goitre nodular region
6	1337/1339	CH_2/CH_3 wagging, twisting and/or bending mode of collagens, lipids, nucleic acid, and tryptophan	Goitre nodular region
7	1552–1585	Tryptophan ν(C=C), tryptophan (protein assignment)	Goitre adjacent tissue

[a] *cf.* also peak assignment numbers in Fig. 2.

Results and discussion

For the analysis and differentiation of the pathologies, it was necessary to conjugate the spectra in different forms. Fig. 2 represents the median between the goitre adjacent tissue spectrum (goitre adj) shown in black, and the goitre nodular region spectrum (goitre) shown in grey. The data were disposed in this way because the samples of the tissue adjacent to the injury belong to the control group of this study; however, all of the samples that are theoretically normal would receive a histologic report of adenomatous goitre. As the doubt between normal thyroid and adenomatous goitre regarding histology and cytology is real and the articles about the real differentiation of

Table 3 Relevant vibrational modes in the differing of adenomatous goitre in comparison to follicular adenoma and follicular carcinoma[10]

Peak (cm^{-1})		Assignment	Pathology
1[a]	500–840	Disulfide bridges, nucleic acids, and nucleotides	Follicular carcinoma Follicular adenoma Goitre nodular region
2	856	Amino acid side chain vibrations of proline and hydroxyproline, as well as a (C–C) vibration of the collagen backbone; hydroxyproline (collagen type I)	Follicular adenoma Goitre nodular region Follicular carcinoma
3	937	Proline, hydroxyproline, ν(C–C) skeletal of collagen backbone	Follicular adenoma Goitre nodular region Follicular carcinoma
4	960	Symmetric stretching vibration of PO_4^{3-}; calcium phosphate stretch band; quinoid ring in-plane deformation	Follicular adenoma Follicular carcinoma Goitre nodular region
5	1095	Lipids, C–N, and PO^{2-} in nucleic acids	Follicular carcinoma Follicular adenoma
6	1208	ν(C–C_6H_5), tryptophan, phenylalanine, tryptophan, A, T (ring breathing), and amide III	Goitre nodular region Follicular adenoma Follicular carcinoma
7	1258–1290	Amide III, adenine, cytosine	Follicular carcinoma Goitre nodular region
8	1315–1339	Tryptophan CH_2/CH_3 wagging, twisting and/or bending mode of collagens and lipids, CH_2/CH_3 wagging and twisting mode in collagen, nucleic acid and tryptophan	Follicular carcinoma Goitre nodular region Follicular adenoma

[a] *cf.* also peak assignment numbers in Fig. 6.

Table 4 Relevant vibrational modes of the adenomatous goitre in comparison to the papillary carcinoma and follicular carcinoma[10]

Peak (cm^{-1})		Assignment	Pathology
1[a]	500–840	Disulfide bridges, nucleic acids, nucleotides	Follicular carcinoma Papillary carcinoma Goitre nodular region
2	856	Amino acid side chain vibrations of proline and hydroxyproline, as well as a (C–C) vibration of the collagen backbone; hydroxyproline (collagen type I)	Papillary carcinoma Goitre nodular region Follicular carcinoma
3	1095	Lipids, C–N, and PO^{2-} in nucleic acids	Follicular carcinoma
4	1208	ν(C–C_6H_5), tryptophan, phenylalanine, tryptophan, A, T (ring breathing), and amide III	Papillary carcinoma Goitre nodular region Follicular carcinoma
5	1258–1290	Amide III, adenine, cytosine	Follicular carcinoma Papillary carcinoma Goitre nodular region
6	1315–1339	Tryptophan CH_2/CH_3 wagging, twisting and/or bending mode of collagens and lipids, CH_2/CH_3 wagging and twisting mode in collagen, nucleic acid and tryptophan	Follicular carcinoma Goitre nodular region Papillary carcinoma
7	1585	C=C bending mode of phenylalanine	Goitre nodular region Papillary carcinoma

[a] *cf.* also peak assignment numbers in Fig. 7.

both are scarce, this study also must verify the difference between both tissues in the FT-Raman spectroscopy.

In Table 2, the relevant vibrational modes are described for the differentiation of the adjacent tissue to the injury and nodular goitre region. The main peaks, their assignments (based on ref. 10), and the corresponding pathologies are show in the second, third and fourth columns, respectively.

Important results were obtained by the statistical analysis by fundamentally using the analysis of the main components of the spectra, associated with the cluster analysis and linear discriminative analysis. The values for each component are expressed in Table 6.

In Table 7, the number of spectra per cluster (and the sample percentage per cluster) is shown when PC1 and PC2 were submitted to cluster analysis. The classification performed by clusters is justified by the fact that there are two groups of injuries in the analysis, and in this way, it is possible to verify whether the groups are similar or distinct. The corresponding dendrogram is shown on Fig. 3. Eighty five per cent of all spectra grouped on Cluster 1 and the remaining on Cluster 2. Cluster 1 has 24 spectra of goitre adjacent tissue (73%) and 27 spectra of nodular region (100%). Cluster 2 has 9 spectra of goitre adjacent tissue (27%). Thus there is a very significant admixture of these two kinds of tissue.

Continuing with the use of the component scores, another way to verify the similarity or distinction of the groups can be done by the Discriminant Analysis (Fig. 4 and Fig. 5).

According to Layfield *et al.*,[8] there are studies and criteria that attempt to separate the follicular neoplasms of the hyperplastic nodules and colloid goitre, but the criteria to differentiate hyperplasias and nodular goitre from the normal thyroidal tissue are seldom discussed in the literature. Colloidal goitre is diagnosed when there is abundant colloid but significant injuries do not exist. Similarly, hyperplastic nodules or adenomatous nodules are diagnosed by small amounts of colloid and a lack of superior degrees of injuries.[8]

In accordance with the obtained results, there are some biochemical alterations between the two kinds of tissue, injury adjacent area and adenomatous goitre central area. These alterations were observed through the difference between the vibrational modes that compose the spectra (Table 2); however, according to the statistical analysis, these spectral modifications are not significant enough to represent a relevant separation between them.

By the cluster analysis, represented in the dendrogram in Fig. 3, a 70% similarity rate among all spectra is represented. By the discriminant analysis (Fig. 5 and Table 8), the general percentage of classification among the spectra was 58.3%, which was a low classification percentage.

The data described justify the statement of Layfield *et al.*[8] that adenomatous goitre is a hyperplasia, with no considerable

Table 5 Vibrational mode of T3 and T4 hormones, as well as goitre adjacent tissue, goitre nodular region and papillary carcinoma[10,11]

Peak (cm^{-1})		Assignment	Pathology or hormones
1[a]	600	Nucleotide conformation	T3 Goitre adjacent tissue Goitre nodular region Papillary carcinoma
2	618	C–C twisting (protein)	T3 Goitre adjacent tissue Goitre nodular region Papillary carcinoma
3	722	DNA; β(15)	T4 T3 Papillary carcinoma Goitre nodular region Goitre adjacent tissue
4	782	DNA; NH_3 + wag	T4 T3 Papillary carcinoma Goitre nodular region Goitre adjacent tissue
5	820–830	Protein band; structural protein modes of tumours; proteins, including collagen I; α/β ring deformation	T4 T3 Goitre nodular region Goitre adjacent tissue Papillary carcinoma
6	856	Amino acid side chain vibrations of proline and hydroxyproline, as well as a (C–C) vibration of the collagen backbone; hydroxyproline (collagen type I); β(12)	T4 Goitre nodular region Papillary carcinoma Goitre adjacent tissue
7	1030	Phenylalanine of collagen; ν(C–C) skeletal, keratin (protein); δ(C–H), phenylalanine (protein); α(9)	T3 Goitre nodular region Goitre adjacent tissue Papillary carcinoma
8	1130	C–C skeletal stretch transconformation; phospholipid structural changes (*trans versus gauche* isomerism); $\delta(OH_{in\text{-}phase})$	T3 Goitre adjacent tissue Goitre nodular region Papillary carcinoma
9	1180	Cytosine, guanine; ν(Cβ-O)	T3 T4 Goitre adjacent tissue Goitre nodular region Papillary carcinoma
10	1239	Amide III; ν(C–O)(α)/(C–$OH_{out\text{-}of\text{-}phase}$)	T4 T3 Goitre adjacent tissue Goitre nodular region Papillary carcinoma
11	1290	Cytosine; β(6)	T3 Goitre adjacent tissue Goitre nodular region Papillary carcinoma
12	1560	Tryptophan α(1); α(1)−β(2); β(2)	T4 Goitre adjacent tissue Goitre nodular region Papillary carcinoma
13	1582	δ(C=C), phenylalanine; β(2); β(2)+α(1); β(1)−α(1)	T3 T4 Goitre adjacent tissue Goitre nodular region Papillary carcinoma
14	1598	C=N and C=C stretching in quinoid ring β(1); β(1); β(1)+α(1)	T3 Goitre adjacent tissue Goitre nodular region Papillary carcinoma

[a] *cf.* also peak assignment numbers in Fig. 14.

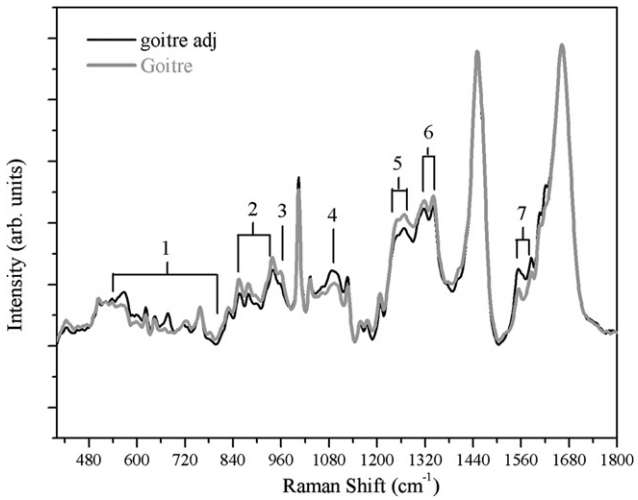

Fig. 2 Median between the spectra of the goitre adjacent tissue (black line) and the nodular region goitre (grey line).

Table 6 Eigenvalue PCA of goitre adjacent *vs.* goitre

Goitre adjacent *vs.* goitre	Eigenvalue	Variability (%)	Accumulated (%)
PC1	56.8	94.8	
PC2	1.3	2.1	96.9
PC3	0.381	0.6	97.5
PC4	0.321	0.5	98.0

Table 7 Number of spectra per cluster and the distance (Linear Discriminant Analysis) in the goitre adj. *vs.* goitre comparison

Goitre adjacent *vs.* goitre	Quantity	Distance
Cluster 1	51 (85%)	0.332
Cluster 2	9 (15%)	

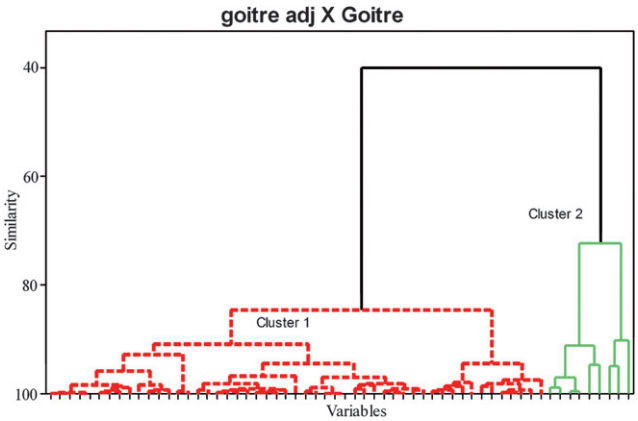

Fig. 3 Dendrogram figure with cluster analysis of the adjacent tissue and goitre nodular region.

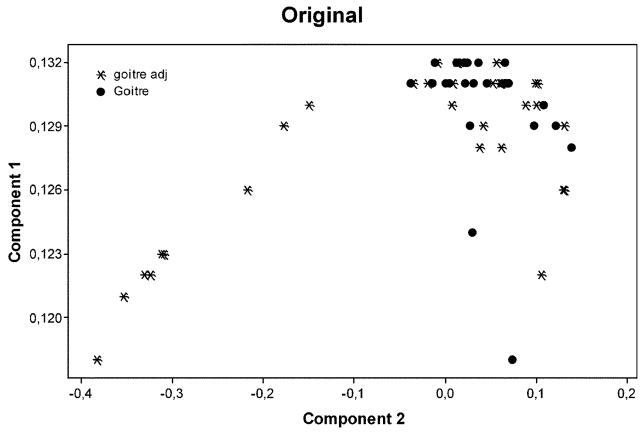

Fig. 4 Chart of the dispersion of groups in the original classification for the adjacent tissue and goitre nodular region.

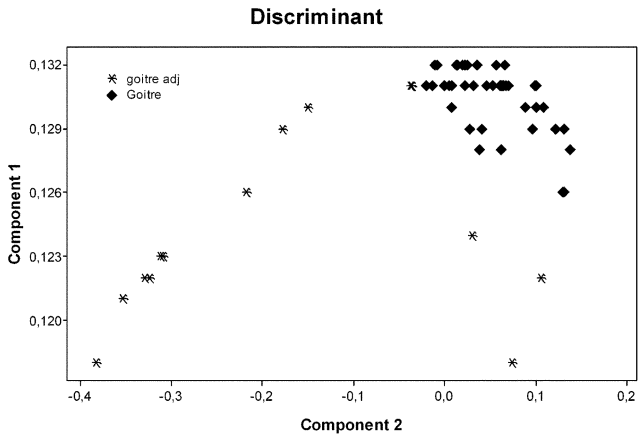

Fig. 5 Chart of the discriminant analysis for the adjacent tissue and goitre nodular region.

Table 8 Classification percentage of the discriminant function in goitre adj. *vs.* goitre

Correct classification	
Goitre adj	33%
Goitre	88.9%
General	58.3%

cellular alterations; this also justifies the similarity between normal thyroid and adenomatous goitre, or adjacent and central tissues of a goitre injury. Alcântara-Jones *et al.*[9] developed an observational study to verify the cytologic standard of the normal thyroidal tissue obtained through aspiration and non-aspiration punctures in corpses, in which an anatomic dissection of the thyroid was carried out and the cytoaspiration performed in 38 cases. Two pathologists, not knowing the correspondence between cytology and histology, in a double-blind study, analysed the smears and histologic cuts. The normal thyroid was given a cytologic diagnosis of adenomatous goitre in 70.4% of cases for one observer and 92.6% for the other. It can be concluded that the cytologic aspect of the normal thyroid in corpses was similar to the adenomatous goitre.[9] This study reflects very well the doubt related to the cytology and histopathology of the thyroid, where not even the normal tissue can be differentiated from the pathologic tissue, making it very difficult to merge. In addition, this justifies the fact that head/neck doctors defend the total thyroidectomy, considering that the partial thyroidectomy is a risky method.

In this study, it was also concluded that there is similarity between the normal thyroid and the adenomatous goitre, as the samples also received a histologic report of adenomatous goitre and the spectra did not separate them in a relevant manner. As a result, uniting the 11 samples of injury adjacent tissue and the 9 samples of goitre nodular area, we formed a group of 20 samples of adenomatous goitre.

Another difficulty for the histology is to differentiate the 'follicular standard'; that is, it is difficult to note the difference between adenomatous goitre, follicular adenoma and follicular carcinoma. In Fig. 6, the black line represents the median of the adenomatous goitre spectra, the grey line represents the median of the follicular adenoma spectra and the dark grey line represents the median of follicular carcinoma spectra.

Table 3 presents the differences between the vibrational modes of these pathologies. Due to the low number of samples, justified by the low occurrence of follicular carcinoma, the statistical analysis of this conjugation was not performed. However, it is important to point out the spectral difference and biochemical modifications present in the spectra of the tissues analysed in this study.

According to Table 3, it can be noted that some peaks appear in all three spectra; that is, the biochemical compositions are nearly the same in all three tissue types, although with different intensities among them. These regions could be similar to those considered characteristic of the normal thyroidal tissue. However, there are also characteristic peaks for only one or two types of injuries, those being the modes of more relevance to differentiate the pathologies for they are exclusive and representative peaks of tissue alteration. It is important to draw attention to the 1095 cm^{-1} band which is characteristic of the

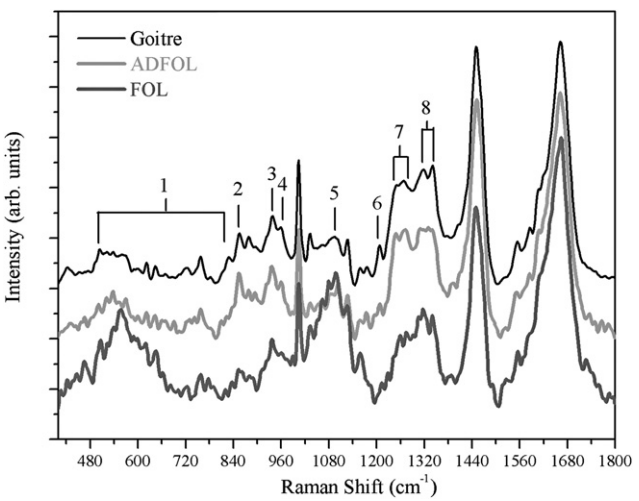

Fig. 6 Median of the adenomatous goitre spectra (black line), follicular adenoma (grey line) and follicular carcinoma (dark grey line).

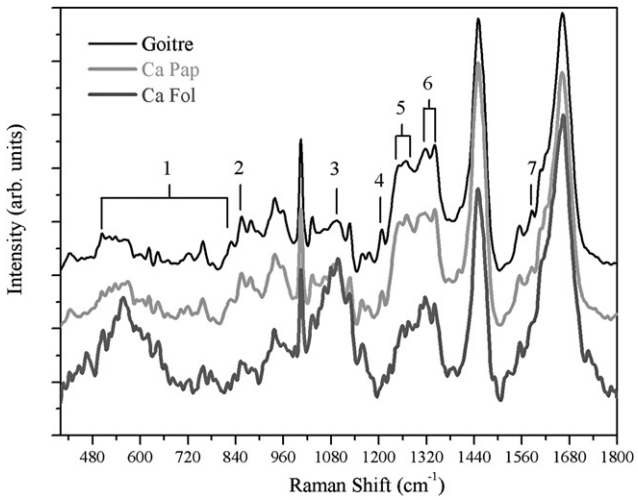

Fig. 7 Median of the adenomatous goitre spectra (black line), papillary carcinoma (grey line) and follicular carcinoma (dark grey line).

follicular carcinoma and follicular adenoma tissues since it did not appear on the goitre nodular region.

The follicular adenoma, on the other hand, has peaks with high intensity at 856, 937, and 960 cm^{-1}. The characteristic peaks for follicular carcinoma are from 500 to 840, 1095, 1258–1290, and 1315–1339 cm^{-1}.

Another important point for medicine and histology would be the greater understanding of malignant and benign injuries, since many times the histologic report relates malignancy suspicion, causing an inconclusive diagnostic. The consistency of the report is essential for the medical conduct and prognosis of the disease. According to the point exposed, the data were conjugated to analyse the adenomatous goitre, papillary carcinoma and follicular carcinoma (Fig. 7 and Table 4).

Proceeding with the analysis to separate the benign and malignant injuries, the multivariate statistical methods were used for the differentiation. In the first analysis, samples of adenomatous goitre and papillary carcinoma (PAP) were studied due to the higher amount of samples present in each group. Lastly, an analysis of all the samples was performed: adenomatous goitre, follicular adenoma, follicular carcinoma and papillary carcinoma (benign group *vs.* malignant group).

By the analysis of the cluster using the main components presented in Tables 9 and 10, it can be noted that the distance between the clusters decreased when we aggregated the spectral data of all kinds of tissues. Tables 11 and 12 demonstrate the number of spectra per cluster, which can also be observed in the dendrogram in Fig. 8 and Fig. 9. In Table 11, the distance was 0.281, while in Table 12 the result was 0.262, showing the diminishing of the spectral spread, especially in the analysis of

Table 9 Eigenvalue of the PCA of goitre *vs.* PAP

Goitre *vs.* PAP	Eigenvalue	Variability (%)	Accumulated (%)
PC1	69.9	94.6	
PC2	1.5	2.1	96.7
PC3	0.604	0.8	97.5
PC4	0.396	0.5	98.0

Table 10 Eigenvalue of the PCA of benign *vs.* malignant

Benign *vs.* malignant	Eigenvalue	Variability (%)	Acumulated (%)
PC1	75.1	93.9	
PC2	2.2	2.7	96.6
PC3	0.636	0.8	97.4
PC4	0.414	0.5	97.9

Table 11 Quantity of spectra per cluster and its distance in goitre *vs.* PAP

Goitre *vs.* PAP	Quantity	Distance
Cluster 1	62 (84%)	0.281
Cluster 2	12 (16%)	

Table 12 Quantity of spectra per cluster and its distance in benign *vs.* malignant

Benign *vs.* malignant	Quantity	Distance
Cluster 1	65 (81%)	0.262
Cluster 2	15 (19%)	

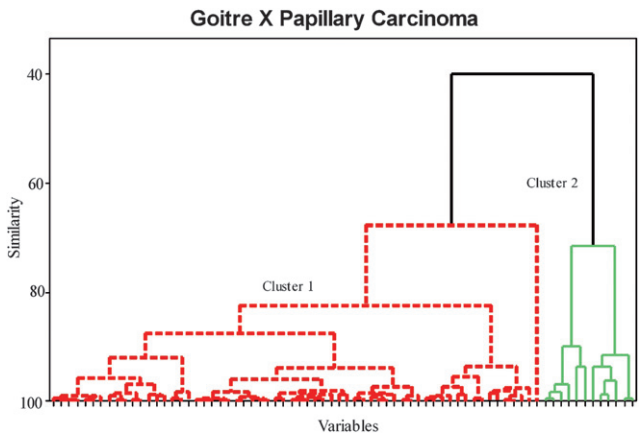

Fig. 8 Dendrogram with the cluster analysis of the adenomatous goitre and papillary carcinoma.

the malignant *versus* benign injuries (Fig. 9). A separation was reached with 73.37% similarity. In the dendrogram of Fig. 8, Cluster 1 has 51 of goitre (85%) and 11 spectra of papillary carcinoma (78%). Cluster 2 has 9 spectra of goitre (15%) and 3 of papillary carcinoma (22%). In the dendrogram of Fig. 9 Cluster 1 has 51 spectra of goitre (85%), 3 spectra of papillary carcinoma (22%), 3 of follicular adenoma (100%) and 11 spectra of papillary carcinoma (78%). Cluster 2 has 9 goitre spectra (15%), 3 spectra of papillary carcinoma (22%) and 3 spectra of follicular carcinoma (100%).

Fig. 10 and Fig. 11 show the dispersion of groups in the original classification and discriminant analysis, respectively for the goitre and papillary carcinoma. The use of these variables creates an 'index' or 'discriminant function' that represents, with parsimony, the difference between the groups. Fig. 12 and Fig. 13 represent the same analysis for benign and malignant groups.

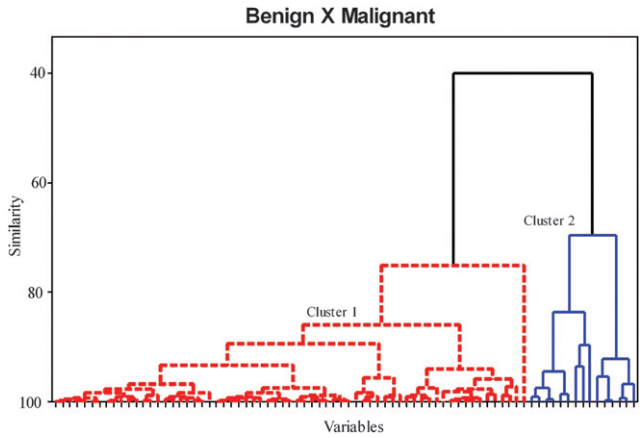

Fig. 9 Dendrogram of the cluster analysis to separate the malignant and benign injuries.

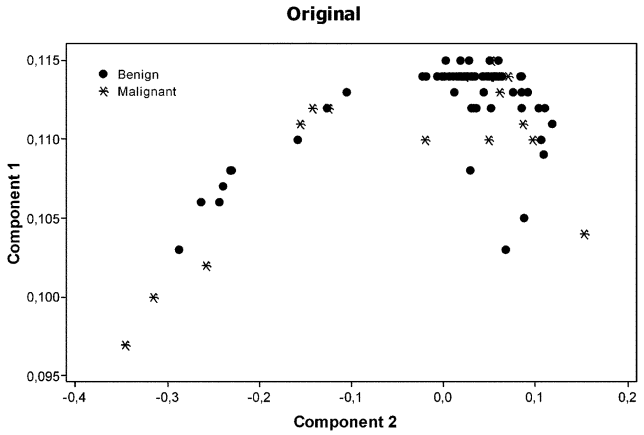

Fig. 12 Chart of the dispersion of groups in the original classification for the benign and malignant injuries.

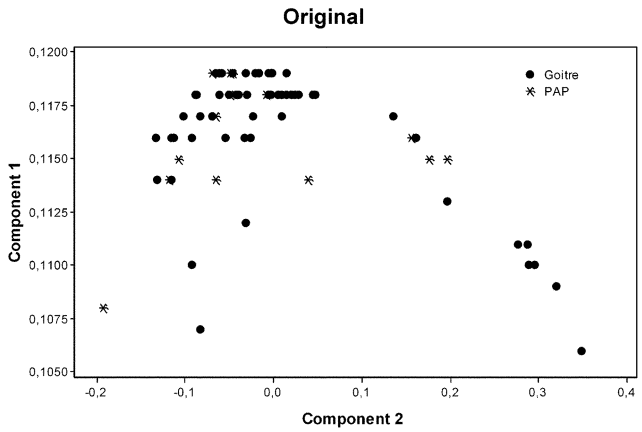

Fig. 10 Chart of the dispersion of groups in the original classification for the goitre and papillary carcinoma.

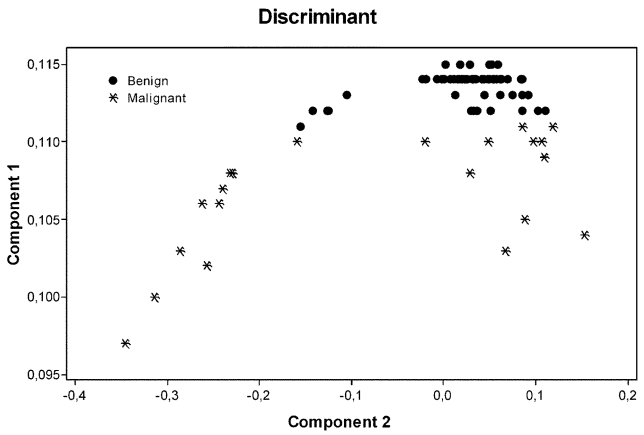

Fig. 13 Graphic of the discriminant analysis between benign and malignant injuries.

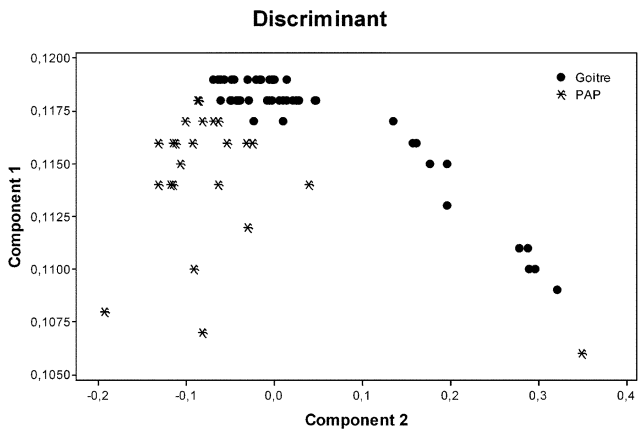

Fig. 11 Graph of the discriminant analysis of the adenomatous goitre and papillary carcinoma.

Table 13 Classification percentage of the discriminant function in benign *vs.* malignant

Correct classification	
Benign	79.4%
Malignant	47.1%
General	72.5%

Table 14 Classification percentage of the discriminant function in goitre *vs.* PAP

Correct classification	
Goitre	70.0%
PAP	42.9%
General	64.9%

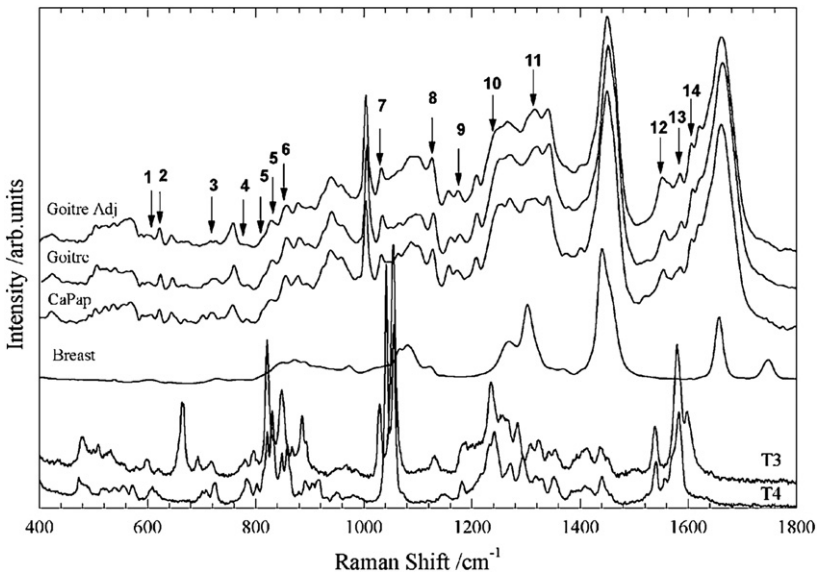

Fig. 14 Median of the spectra of T3 and T4 hormones – the black and dark grey spectral lines in the lower part of the graph. Median of the spectra for the goitre adjacent tissue (Goitre Adj), goitre nodular region (Goitre) and papillary carcinoma (CaPAP) in the upper part of the graph. Also displayed is a typical breast tissue spectra (Breast).

Comparing the statistical methods, the best result was obtained by the discriminant analysis, since when analysing the clusters and its dendrograms, the classification was not favourable. Important data that need to be verified are the individual percentages of each group. In the benign *vs.* malignant analysis, these percentages were higher, reaching nearly 80% in the benign injuries (Table 13).

Analysing Tables 8, 13 and 14 with the correct classification percentages for the general group, it is clear that with the conjugation between the groups, this percentage increased. For the groups goitre adjacent tissue *versus* goitre nodular region, a result of 58.3% of correct classification was obtained; this percentage was low, and it was not possible to discriminate the FT-Raman spectra of these two groups. Between goitre (nodular region and periphery) and papillary carcinoma, the correct classification index was 64.9%, which was considered good.

However, relevant results were obtained in the analysis of the spectra in the benign tissues (goitre and follicular adenoma) *versus* malignant tissues (papillary and follicular carcinomas) analysis, for which the percentage was 72.5%, which was considered very good.

It was also verified that it is also important to analyse the hormones, considering that the main function of this organ is to synthesise T3 and T4. These components are utilised as polypeptidic extracellular reserves in the colloid inside the follicular lumen of the thyroidal cells. The characteristic spectra for the T3 and T4 synthetic hormones were collected for comparison with the spectra of goitre adjacent tissue, goitre nodular goitre and papillary carcinoma (Fig. 14). To clearly ascribe the hormone vibrational bands, a typical breast tissue spectrum was also displayed in Fig. 14 where the T3 and T4 presence is not significant. Table 5 presents the vibrational bands of the T3 and T4 hormones correlated to the gland tissue.

The spectra in Fig. 14 were included to enable the analysis of the hormone peaks with similar vibrations to those found on the biological tissues. The ligation frequency or atomic vibrations normally merge, forming spectra that are difficult to understand. For that reason, the many probable modes for each region were related as hypotheses; for example, the region of 722 cm^{-1} for biological tissues could be attributed to the DNA vibrational mode or mode β(15) of hormones T3 and T4 present on colloids or follicles. It is also important to verify the intensity of these coincident peaks when it is known that the level of these hormones can vary according to the pathology.

Conclusions

The heterogeneity of the thyroid gland should be noted in this study. In the same sample, two or three injuries were analysed together, which makes it difficult to cytopathologically and histopathologically report on the injuries when a consolidated difference between them cannot be found. This difficulty was also present in the FT-Raman spectroscopy method, suggesting the use of this technique as a complement of the diagnosis of pathologies.

By the discriminative analysis of the spectra obtained through the FT-Raman spectroscopy method, the goitre adjacent tissue and goitre nodular region are considered similar, as described by the histology, due to the low classification percentage. Uniting these data (goitre adjacent tissue and goitre nodular region), another group was formed, total goitre *versus* papillary carcinoma, and there was a good discrimination between goitre and papillary carcinoma. The classification index became bold and considerable when the spectra of follicular adenoma and follicular carcinoma were included. Therefore, benign injuries (goitre adjacent tissue, goitre nodular region and follicular adenoma) and malignant injuries (follicular and papillary carcinoma) could be classified.

Regarding the difficulty in differentiating what is called the 'follicular standard', some differences were noted in the spectral conformation of the adenomatous goitre group compared to the follicular adenoma and follicular carcinoma group. The follicular adenoma, on the other hand, has peaks with high intensity at 856, 937, and 960 cm^{-1}. The characteristic peaks for follicular carcinoma are from 500 to 840, 1095, 1258–1290, and 1315–1339 cm^{-1}.

These data are nothing but the native ligation nature modifications present in each injury, which brings relevant data to differentiate and complement the 'follicular standard' studies.

The gland tissue is in fact very complex. Any modification or mutation that may occur, combined with the hormone synthesis, interferes in the spectral analysis, as it generates clashing information due to the high number of functional groups vibrating at the same time. However, in Fig. 14, it is possible to verify the hormones' vibrating peaks which, in the future, will allow the dosage through the FT-Raman spectroscopy method and at the same time study its isolated interference on the tissues.

Acknowledgements

The authors thank Prof. Anita Mahadevan-Jansen for fruitful discussions and also for the background subtraction routine. The authors also thank for Brazilian agencies FAPESP (01/14384-8) and CNPq (301018/2006-5).

References

1 *Basic & Clinical Endocrinology*, ed. F. S. Greenspan and G. J. Strewler, Appleton and Lange, Stamford, 1997.
2 S. L. Robbins, R. S. Cotran and V. Kumar, *Pathologic Basis of Disease*, WB Saunders, Philadelphia, 1984.
3 S. Matsuo, L. Martins, S. G. Leoni, D. Hajjar, J. C. Ricarte-Filho, K. N. Ebina and E. T. Kimura, *Arq. Bras. Endocrinol. Metabol.*, 2004, **48**, 114–124.
4 P. Rout and S. Shariff, *Cytopathology*, 1999, **10**, 171–179.
5 K. Z. Liu, C. P. Schultz, E. A. Salamon, A. Man and H. H. Mantsch, *J. Mol. Struct.*, 2003, **661–662**, 397–404.
6 C. Hedinger, E. D. Williams and L. H. Sobin, *Histological typing of thyroid tumours*, Springer-Verlag, WHO International Histological Classification of Tumors, Berlin, 1998.
7 R. A. Bitar, H. S. Martinho, C. J. T. Criollo, L. N. Z. Ramalho, M. M. Netto and A. A. Martin, *J. Biomed. Opt.*, 2006, **11**, 054001.
8 L. J. Layfield, T. Wax and C. Jones, *Cancer Cytopathol.*, 2003, **99**, 217–222.
9 D. M. Alcântara-Jones, J. S. Miranda, S. S. Matos, C. M. P. Queiroz, L. M. B. Aráujo, M. A. V. Rêgo, A. M. Santana, B. F. Lessa and C. E. M. Nunes, *J. Bras. Patol. Med. Lab.*, 2006, **42**, 45–50.
10 Z. Movasaghi, S. Rehman and I. U. Rehman, *Appl. Spectrosc. Rev.*, 2007, **42**, 493–541.
11 R. M. S. Álvarez, R. N. Farías and P. Hildebrandt, *J. Raman Spectrosc.*, 2004, **35**, 947–255.

